Measurement 172 (2021) 108859

Contents lists available at ScienceDirect

Measurement

journal homepage: www.elsevier.com/locate/measurement

Molybdenum strip test experiments and simulations at various temperatures to determine friction coefficients

Frantisek Brumercik [a,*], Ronald Bastovansky [a], Michal Lukac [a], Adam Glowacz [b]

[a] University of Zilina, Mechanical Engineering Faculty, Departement of Design and Machine Elements, Univerzitna 1, 010 26 Zilina, Slovakia
[b] AGH University of Science and Technology, Faculty of Electrical, Engineering, Automatics, Computer Science and Biomedical Engineering, Department of Automatic Control and Robotics, Al. A. Mickiewicza 30, 30-059 Kraków, Poland

ARTICLE INFO

Keywords:
Molybdenum
Drawbead
Strip test

ABSTRACT

The aim of the presented study was to perform the strip test of 0.5 mm thick molybdenum strip specimens by various simulated drawbead heights from 2 mm up to 6 mm and various temperatures from 20 °C up to 320 °C to obtain friction coefficients between the molybdenum strip and steel cylinders built-in the developed test device simulating the drawbead. The friction coefficients between the dry and lubricated molybdenum strip and the steel cylinders simulating the drawbeads were obtained by changing its value in the bilinear friction model and matching the holder drawing force and the drawbead restraint force curves achieved during the tests and the simulations. The increasing temperature of molybdenum strip led to reduced holder drawing force and drawbead restraint force and increased friction coefficient because of the decrease of molybdenum strip yield strength and the increase of surface contact between molybdenum sheet and the testing tool at elevated temperature.

1. Introduction

Improvement of production technology of optical and laser single crystals from the melt as leucosapphire and yttria-alumina garnet (YAG) and the production of them largely determines the success of the most important directions in the development of microelectronics, energy, optoelectronic and laser technology. The wide usage of single crystal sapphire is possible due to its unique properties - high optical uniformity and clarity in a wide range of wavelengths of light, radiation resistance, high mechanical, thermal and dielectric properties. Large demand for sapphire optical products, which are widely used as illuminators, optical windows in aviation and aeronautics, etc. generates the necessity of effective production of high quality industrial crystals. The technology of the crystal growth with the horizontal single crystal sapphire crystallization method, which is also called as the Bagdasarov method (Fig. 1), is a method of growth of the single crystal from a melt of aluminum oxide carried out in a special vacuum system technology at temperatures up to 2150 °C [1,2].

The horizontal method of crystallization requires a special container (also called crucible, crystallization boat, or vessel), which will resists the extreme thermodynamic exposure up to 2150 °C repeatedly without breaking its structural homogeneity. Currently, the containers are made of molybdenum sheet produced by powder metallurgy, e.g. by plastic deformation and sintering procedure with a thickness of 0.5 mm.

Molybdenum (Mo) and its alloys show characteristics such as high melting point, good high-temperature strength, high wear resistance, high thermal conductivity and low resistivity, low coefficient of linear expansion, high elastic modulus, and good corrosion resistance. Based on this, they have irreplaceable functions and application demands in the fields like the defense industry, aerospace, electronic information, energy, chemical defense, metallurgy, and nuclear industry. However, Mo and Mo alloys are hard and brittle materials in nature, so their weldability is generally poor [3]. The production of complicated shapes from thin molybdenum sheets seems less complicated by using deep drawing instead of welding. The mechanical properties of the metallic sheet are an important factor and inadequate consideration of this factor in the design of sheet metal forming manufacturing processes causes buckling, excessive thinning, tearing and wrinkling of the components [4].

The production of the molybdenum containers is carried out usually by careful manually bending of the molybdenum sheet metal cut by the ambient temperature, alternatively supported by a small burner used locally by the complicated corner bends to rise the plasticity of the bent blank. The typical shape of a manually bent single-use molybdenum

* Corresponding author.
E-mail address: brumercikf@fstroj.uniza.sk (F. Brumercik).

https://doi.org/10.1016/j.measurement.2020.108859
Received 17 July 2020; Received in revised form 22 October 2020; Accepted 8 December 2020
Available online 16 December 2020

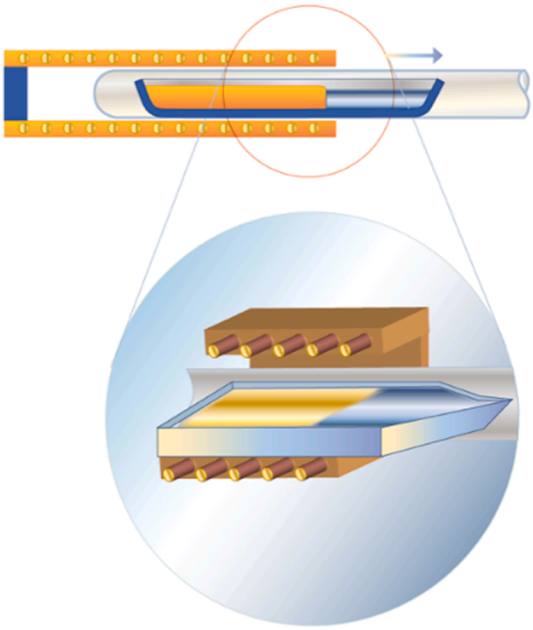

Fig. 1. The principle of the Bagdasarov crystallization method.

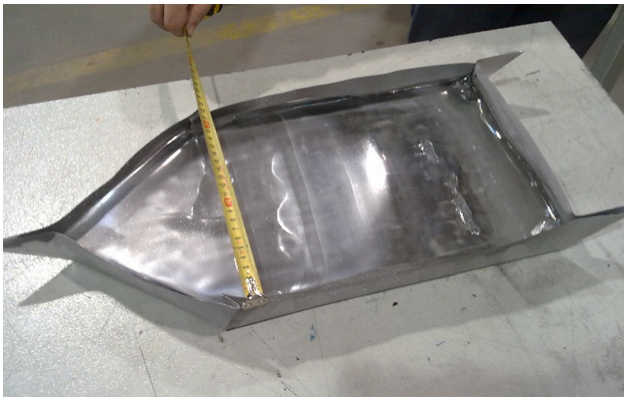

Fig. 2. Manually produced crucible with the sapphire ingot after the crystallization process.

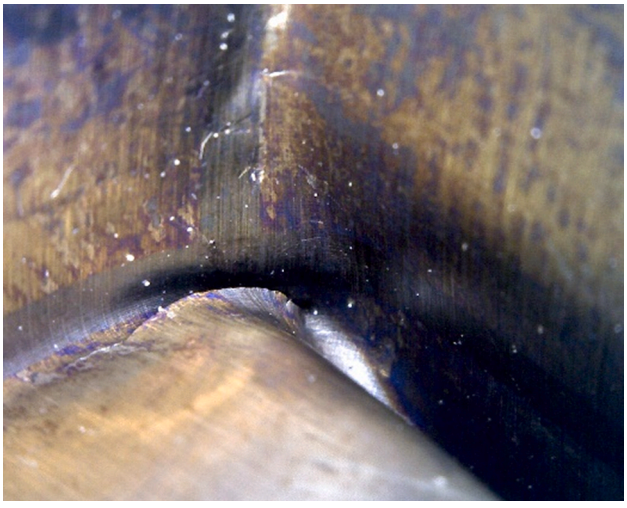

Fig. 3. Crack of the manually produced molybdenum container in the corner region.

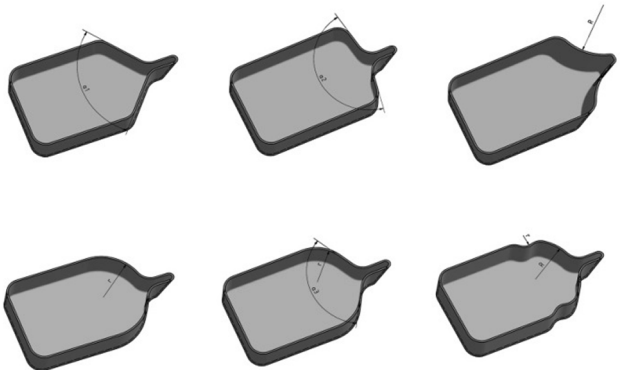

Fig. 4. Possible shapes of the molybdenum crystallization container.

container with dimensions of 450 × 220 × 35 mm filled with the sapphire ingot after the crystallization process by the Bagdasarov method is shown in Fig. 2.

The technology of the manual production of the molybdenum containers leads to uneven shapes and dimensions of each produced crucible and it is not suitable for the mass production. It is caused by adverse deformation properties of the molybdenum sheet, which has a great affinity to oxygen. Thin-walled containers have unbalanced curved corners with various imperfections, which cause complications by the melting process and by the release of the sapphire ingot from the crucible after crystallization, which is usually accompanied by destruction of the container. The containers produced with such technology are prone to cracks, which occur most often in the corner regions (Fig. 3). The unidentified cracks can cause fatal damages during the melting process by subsequent leakage of the melt with a temperature of 2100 °C in a vacuum chamber space of the sapphire crystallization system [5].

The problems of the molybdenum container production led to the idea to develop a technological device for a deep drawing of the containers from thin molybdenum sheets with the possibility to control the drawing process. The mastery of the production technology of such special container made from thin molybdenum sheet is the key to the productive exploitation of horizontal crystallization systems into the engineering practice. The molybdenum drawing properties complicate the mass production of the crucible with a shape, which is difficult especially in its front (crystal seed) area. The possible shapes of the molybdenum containers suitable for the mass production are shown in Fig. 4.

Meng et al developed a device for molybdenum drawing by high temperatures up to 870 °C by the vacuum degree of 10^{-2} Pa with variable blank holding force system [6]. They also performed molybdenum uniaxial tensile tests at the temperatures from 720 to 870 °C to obtain relevant constitutive material equations [7]. Nazaryan and Arakelyan have worked on experiments with lower molybdenum drawing temperatures. They determined, that the maximum degree of molybdenum deformation depends on the temperature-speed modes of deformation, the conditions of friction and the drawing force. The maximum degree of deformation was increased by providing a certain temperature gradient of drawing tools. The temperature was defined to about 300 °C at the outer contour of the work piece and 15 °C on the punch. They also made a crucible of 0.7 mm thick molybdenum sheet with a standard tensile machine without inert gas atmosphere [8].

2. The goals of the performed tests and simulations

The complex shape of the crucible seed area led to the idea to use by its deep drawing the drawbeads commonly used in automotive industry to produce complicated shapes as car sheet metal parts. A computer controlled blank holder could be used to achieve the deformation process control of such complicated structures. The drawbeads can generate

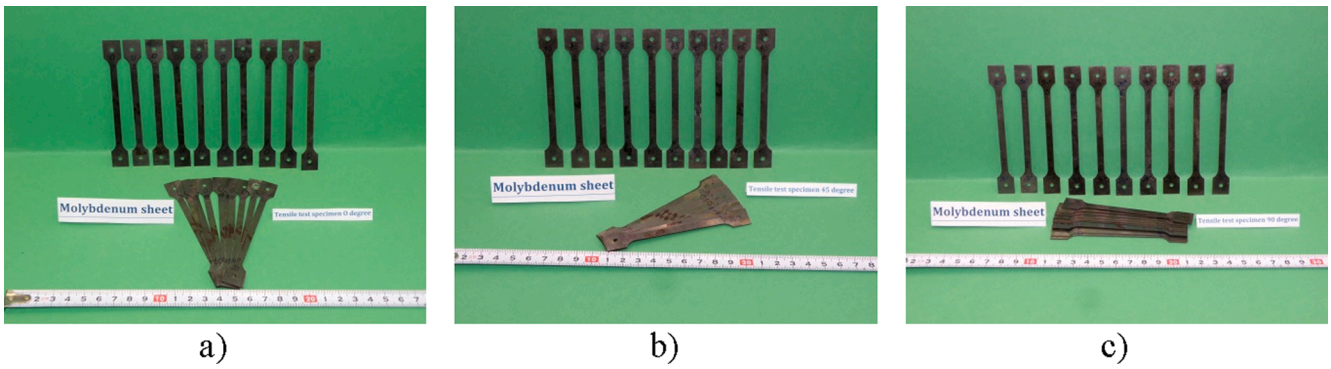

Fig. 5. Tensile test Mo sheet specimen sets with various orientations to rolling direction: a) $\theta = 0°$; b) $\theta = 45°$; a) $\theta = 90°$.

a stable tensile force opposite to the sheet drawing direction by introducing a series of local bending, straitening and reverse bending deformation on the sheet as described by Livatyali et al. [9]. The design and selection of drawbead elements by molybdenum deep drawing requires the determination of sheet drawing characteristics. It is necessary to know the drawbead restraint force (DBRF) and the computer aided holder drawing force (HDF) as the baseline parameters and also the friction coefficients by various drawbead heights and temperatures by dry and lubricated working surfaces to control the drawing process properly.

The controlled deep drawing process presented and performed by Meng et al. [6] by high temperatures puts high demand on materials used by the design of drawing components including the need of vacuum. The results of the deep drawing of molybdenum sheets by lower temperatures without the need of vacuum in a standard drawing machine was described by Nazaryan and Arakelyan [8]. Their research initiated the idea to develop a mechatronic molybdenum deep drawing system working by temperatures up to 400 °C with local heating of the drawn blank and with the possibility of working space inert gas pollution to maintain the molybdenum oxidation described by Martikan et al. [1] and Mitka et al. [10]. Zmindak et al. [11] performed the pilot finite element method (FEM) simulation of molybdenum square cup deep

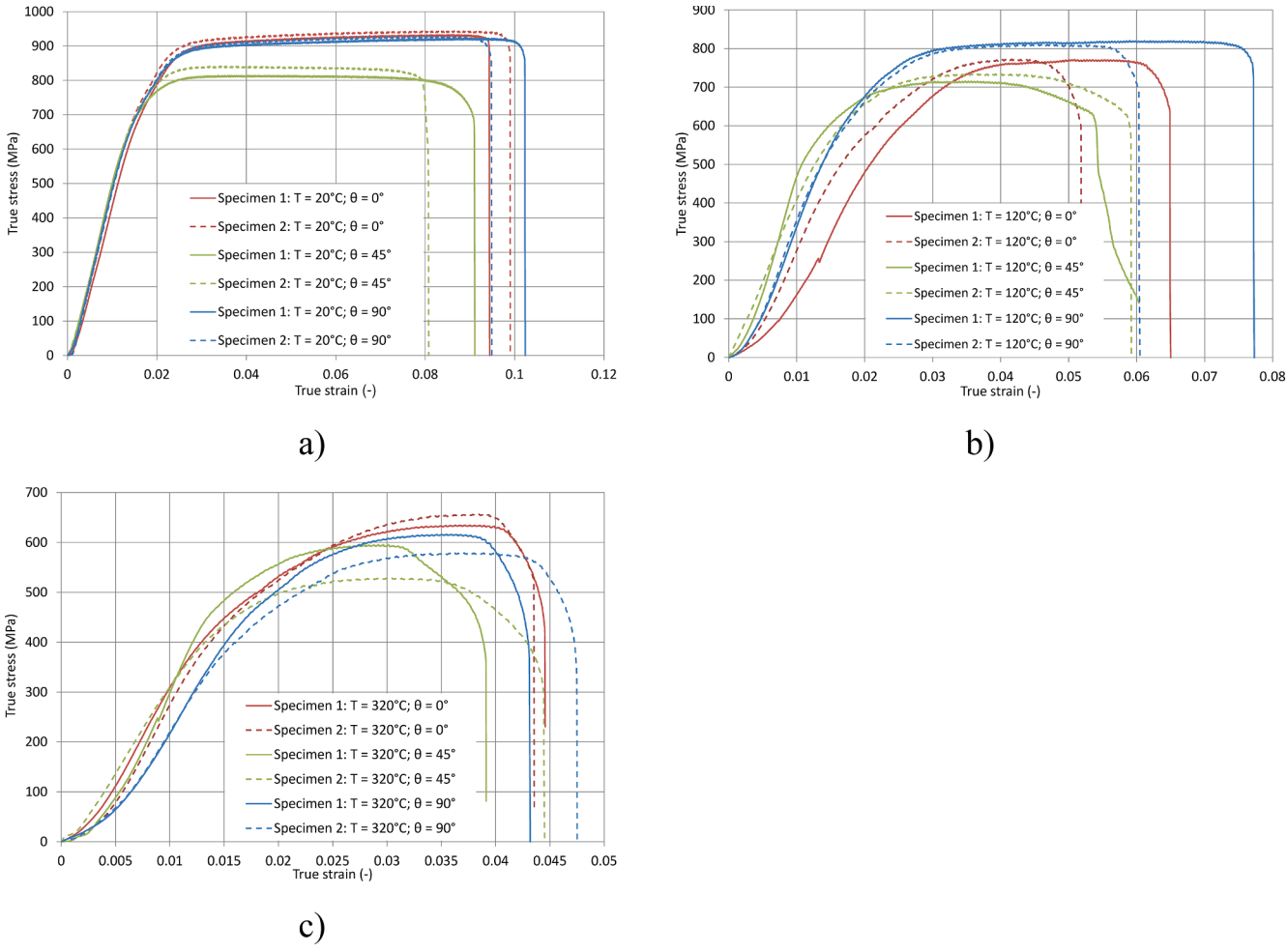

Fig. 6. Uniaxial tensile tests results of molybdenum specimen groups by various temperatures and orientations to rolling direction: a) $T = 20$ °C; b) $T = 120$ °C; c) $T = 320$ °C.

drawing with generic drawbeads. The analyses were done to collect the data for the drawing process control by high temperatures using the material model based on the Meng's work [7] and according the stress analysis applied to production of molybdenum crucible to growth single crystals done by Arab et al. [12] too. However, the friction coefficients used by the simulation were not supported by any experiments. This fact caused the need to perform the strip tests by various temperatures and drawbead heights to obtain a set of frictions coefficients usable by the deep drawing simulations in the drawbead area. The main reason was to continue with simulations based on the work of Zmindak et al. [11] by lower temperatures simulating more complex crucible shapes.

3. Research methodology

Thibaut et al. described the calculation of the molybdenum friction coefficient by the temperatures from 600 to 1000 °C in [13], which was proved by Lin et al. by the inverse calculation of the friction coefficient during the warm upsetting of molybdenum [14]. Meng et al. [15] obtained the values of the friction coefficient of molybdenum at high temperatures by experiments and numerical simulations using the modified Coulomb model. Following the approach of the inverse calculation of the friction coefficient during the warm upsetting of molybdenum and the need to obtain the coefficients of friction for further analyses of a molybdenum container drawing, a test device for the strip test was built [2]. Meng et al. [15] stated, that the drawing force is controlled by the friction at the interface between the cylinder and the strip blank and the magnitude and shape of drawing force curve provide a quantitative information about the coefficient of friction at a certain forming temperature. Analogous to the inverse comparison approach described there, the coefficient of friction at a certain temperatures was obtained via matching the HDF and DBRF curves measured by the experiment with the simulation results in the presented study. The research process was executed in three steps:

1. the uniaxial tests of the molybdenum specimens were done by various temperatures to obtain the material characteristics for the numerical simulations,
2. the strip tests of the molybdenum strips were done by the same temperatures as the uniaxial tests with dry and lubricated contact surfaces,
3. the numerical simulations of the strip tests were performed using the material data obtained by the uniaxial tests. The friction coefficients in the Coulomb bilinear material model were changed in the simulation process until the calculated curves of the drawbead restraint force (DBRF) and the holder drawing force (HDF) matched to the ones gained by the strip test experiments.

3.1. Uniaxial tests

In this study, there was a series of uniaxial tension test performed to obtain the molybdenum sheet flow stress curves by the temperatures T = 20 °C, 120 °C and 320 °C. The specimen sets used during the tests are shown in Fig. 5. The original gauge length of the specimens was $L_0 = 60$ mm and the original cross-sectional area was $S_0 = 2.7832$ mm^2 (0.5 × 5.56 mm).

The used 99.97% Plansee conventional draw-quality molybdenum sheets were cut to specimens oriented at the angles of 0°, 45° and 90° to the rolling direction. The tests were performed on the conventional tensile test machine LabTest 5.20ST by constant strain rate of 0.02 s^{-1}. The results of the tensile tests – the true stress and true strain dependence calculated according to the equations presented by Hosford and Caddell [16], are shown in Fig. 6.

The presented uniaxial tensile tests results of molybdenum specimen groups by various temperatures and orientations to rolling direction show the decrease of the true stress and true strain rates by the rising temperature. The specimens oriented at the angle 45° to the rolling direction show lower values of the tensile strength, hence this orientation is not suitable for further tests. Korolev and Shofman advice already in their early work [17] the usage of sheets, which have been rolled in two mutually perpendicular directions for deep drawing. The specimens from sheets produced by cross rolling along the surface of the sheet have the mechanical properties little distinguished in the two mutually perpendicular directions of rolling, which was confirmed too. The trend of the true stress and true strain rates matches also the results of the uniaxial experiments performed by Meng et al. [7], who tested the molybdenum specimens in the rolling direction at the temperatures from to 993 K to 1143 K at an interval 50 K with strain rates ranging from 0.0005 to 0.02 s^{-1}. The data collected by the uniaxial tensile tests, which served as base by finite element analysis (FEA) material model building, are presented in Tables 1–3.

Table 1
Data from the molybdenum specimen sets uniaxial tensile tests and material model calculations: T = 20 °C.

Specimen set	θ (°)	T (°C)	R_m (MPa)	$R_{p0.2}$ (MPa)	A (%)	n (-)	k (-)
1–0	0	20	938.00	700.00	8.60	0.0778	1135.30
2–0			950.00	700.00	8.80	0.0807	1155.85
Average			944.00	700.00	8.70	0.0793	1145.59
1–45	45		827.00	652.00	8.40	0.0636	968.13
2–45			851.00	651.00	7.60	0.0736	1028.86
Average			839.00	651.50	8.00	0.0686	997.64
1–90	90		942.00	690.00	9.00	0.0818	1147.03
2–90			932.00	690.00	7.00	0.0846	1167.01
Average			937.00	690.00	8.00	0.0829	1155.39
Mean value			889.75	673.25	8.18	0.0748	1074.06

Table 2
Data from the molybdenum specimen sets uniaxial tensile tests and material model calculations: T = 120 °C.

Specimen set	θ (°)	T (°C)	R_m (MPa)	$R_{p0.2}$ (MPa)	A (%)	n (-)	k (-)
3–0	0	120	771.00	576.00	2.80	0.1105	1144.52
4–0			772.00	546.00	2.30	0.1418	1318.11
Average			771.50	561.00	2.55	0.1252	1221.19
3–45	45		715.00	536.00	4.80	0.0907	941.62
4–45			734.00	547.00	3.40	0.1038	1042.59
Average			724.50	541.50	4.10	0.0964	985.72
3–90	90		820.00	592.00	4.60	0.1039	1129.18
4–90			810.00	585.00	3.00	0.1202	1234.49
Average			815.00	588.50	3.80	0.1106	1170.07
Mean value			758.88	558.13	3.64	0.1071	1090.67

Table 3
Data from the molybdenum specimen sets uniaxial tensile tests and material model calculations: T = 320 °C.

Specimen set	θ (°)	T (°C)	R_m (MPa)	$R_{p0.2}$ (MPa)	A (%)	n (-)	k (-)
5–0	0	320	634.00	406.00	2.30	0.1825	1261.98
6–0			656.00	416.00	1.40	0.2341	1781.71
Average			645.00	411.00	1.85	0.2026	1447.41
5–45	45		595.00	441.00	2.80	0.1135	892.80
6–45			530.00	407.00	1.80	0.1202	858.93
Average			562.50	424.00	2.30	0.1157	870.41
5–90	90		578.00	407.00	2.00	0.1523	1048.91
6–90			672.00	469.00	2.00	0.1562	1238.06
Average			625.00	438.00	2.00	0.1544	1143.43
Mean value			598.75	424.25	2.11	0.1471	1082.91

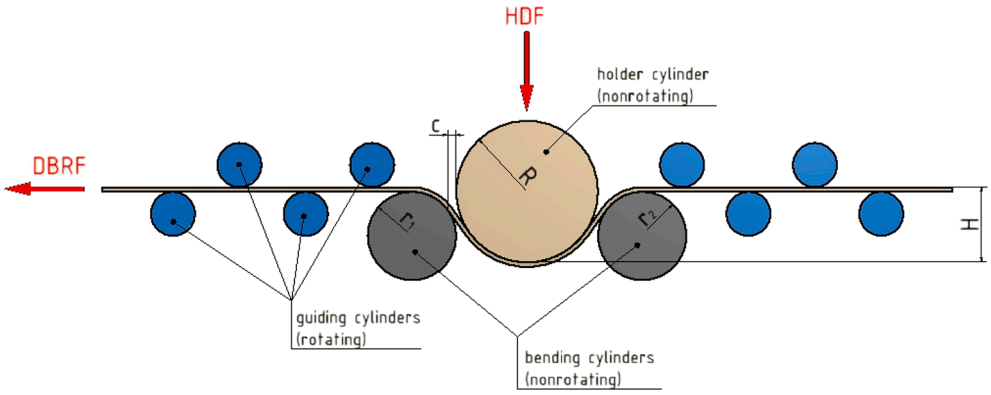

Fig. 7. Baosteel/Sanchez experiment principle.

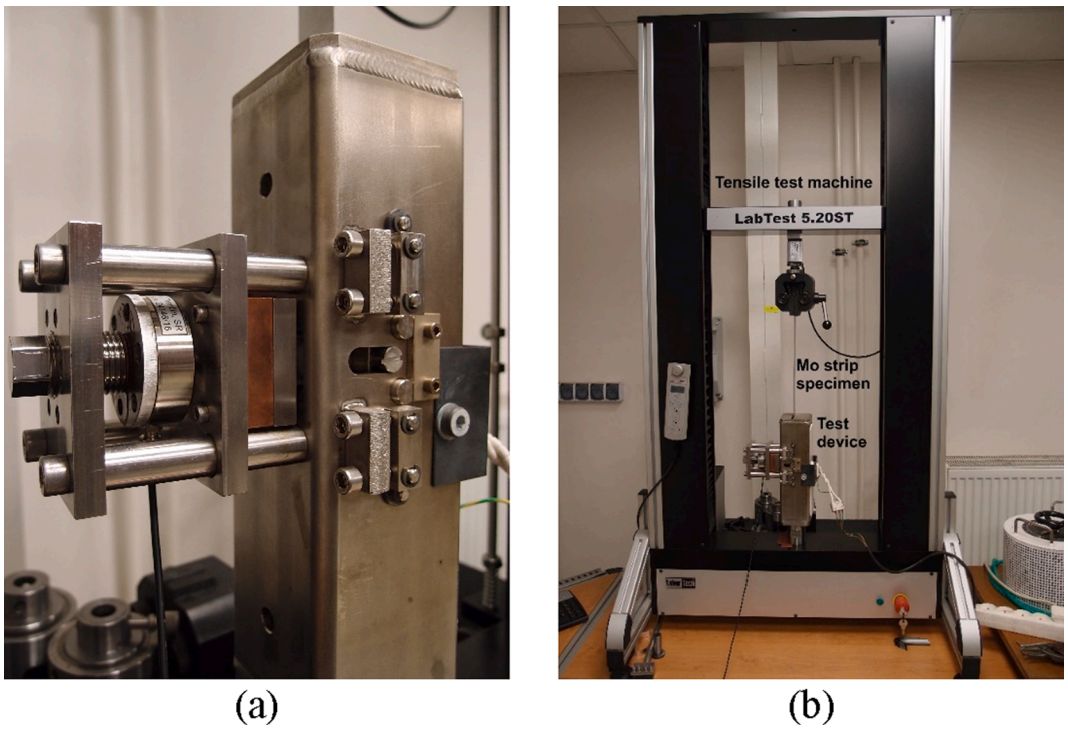

Fig. 8. Strip test device: (a) detail; (b) test configuration in the tensile test machine.

3.2. Strip tests

The common procedures of the strip tests are most common inspired by early work of Nine [18]. Trzepiecinski et al. [19] performed a strip test using a test device built for the usage in a common tensile test machine to obtain the steel sheet friction coefficients by various drawbead hight and surface roughnesses of rollers. Trzepiecinski and Lemu [20] presented also the calculation method of the friction coefficient by a common drawbead strip test procedure performed in first step with free rotatable cylinders and in second step with fixed cylinders mounted at the test device. Leocata et al. [21] studied the influence of the drawbead on the friction, while the friction coefficient is determined before and after the drawbead pass in dependence of the normal pressure.

The behavior of the sheet metal drawbead including the friction coefficients can also be obtained on a test device developed according the Baosteel/Sanchez strip test described by Machalek [22]. The authors developed a test device uses only fixed rollers, hence the force of the free cylinders used in a common calculation of the coefficient of friction cannot be obtained. The value of the friction coefficient is achieved with the inverse method desribed by Meng et al. [15], by the change of its value during the numerical analysis, until the curves of the measured and calculated forces match with each other.

The strip test device developed by Bastovansky et al. [2] is suitable for a common tensile test machine. The device allows to execute the strip test of the sheet metal specimens up to 50 mm wide and 1 mm thick by the maximum temperature of 400 °C. The measured data are the drawbead restraint force (DBRF) and the holder drawing force (HDF) as the baseline parameters for the method of gaining the friction coefficient described above. The experiment principle is shown in Fig. 7.

The radii of the fixed (nonrotating) cylinders were defined as $R = 8$ mm and $r_1 = 5$ mm, the guiding free rotating cylinders have the radius $r = 2{,}5$ mm. All device parts are manufactured from the heat-resistant steel AISI 309/310, that resists the temperatures up to 400 °C applied during the tests. The detail of the strip test device and its test configuration in a common tensile machine is presented in Fig. 8.

The molybdenum sheet sample was put between the guiding valves and clamped to the tensile test machine jaws. The clearance between the

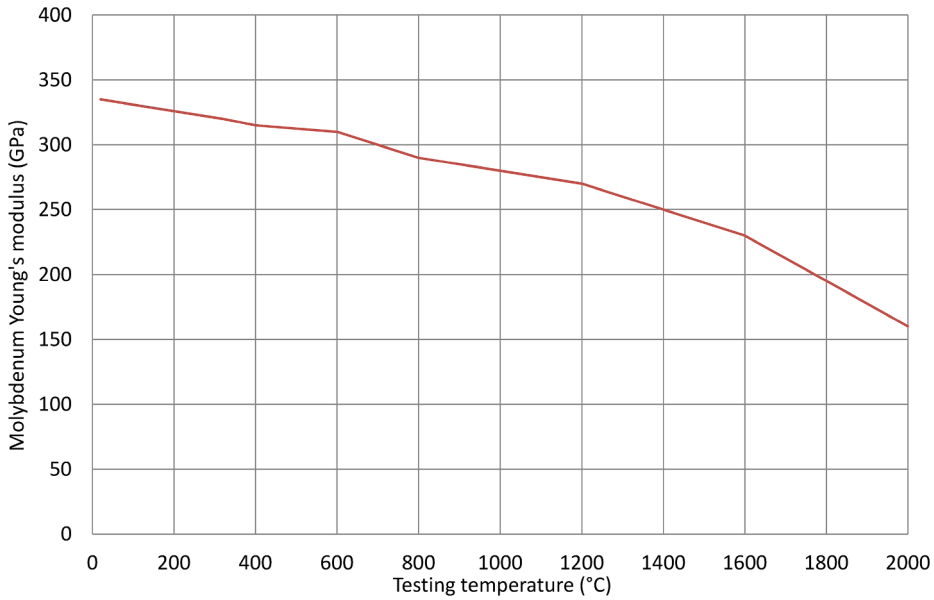

Fig. 9. Molybdenum Young's Modulus temperature dependence.

guiding valves and the blank was then adjusted and the holder cylinder was set up to cause the press offset in the blank – the desired depth H (Fig. 7). The drawbead restraint force (DBRF) was recorded by the measuring system connected to the laptop and the holder drawing force (HDF) was followed on the oscilloscope. The heating was provided by the ceramic heater FFE – 1000 W. The test device was insulated by the insulating coat to prevent the heat leakage. The sensors were equipped with coolers to prevent their damage by higher test temperatures. The temperature was measured on the top and bottom part of the molybdenum blank by a pair of thermocouples.

The tested strips were 20 mm wide and 300 mm long cut from 0.5 mm thick Plansee conventional draw-quality molybdenum sheets produced by the technology of sintered carbides from the nano-powder. The tests were performed by 20 °C, 120 °C and 320 °C according to the uniaxial tensile tests temperatures. The drawbead penetration H was set to 2, 4 and 6 mm selected according the current test conditions. The tests were performed at a conventional tensile test machine LabTest 5.20ST by the constant strip drawing velocity of 30 mm min^{-1} corresponding to the strain rate of 0.02 s^{-1} used also by the uniaxial tensile tests. The cylinders and strips were lubricated with the GLEIT–μ 516 lubricant, which is a homogenous grease without graphite designated also to drawing by high temperatures [23].

3.3. Numerical simulations and data curves matching

A simple 2D strip test model was built in this study to achieve the FEA calculation rapidity. The strip tests were done on specimens cut just parallel to the rolling direction. According the approach described by Kim et al. [24], that is based on the models of the temperature and strain rate dependend material model of molybdenum usable by deep drawing process simulation published by Chang et al. [25], it is assumed the isotropic molybdenum material model is a good approximation for such simplified calculation.

The mean values of the tensile parameters R are determined by the angle of rolling direction $\theta = 0°$, 45°and 90° according the equation used by Trzepiecinski [26]

$$R_{mean} = \frac{R_0 + 2R_{45} + R_{90}}{4} \tag{1}$$

The hardening rules for the FEM model are defined from the mean tensile values based on average specimen groups strength and strain values according to Hollomon equation

Table 4
Molybdenum Young's modulus by various temperatures.

Testing temperature T (°C)	Mo Young's modulus E (MPa)
20	320,000
120	330,000
320	335,000

$$\sigma = k\varepsilon_p^n \tag{2}$$

The strain-hardening exponents n and the strength coefficients k are calculated according to traditional equations from the tensile strength R_m, the elongation after fracture ε_m and the strength by 0.2% elongation $R_{p0,2}$ values described by Zhang et al. [27] as

$$n = \frac{ln\frac{R_m}{R_{p0.2}}}{ln\frac{\varepsilon_m}{0.002}} \tag{3}$$

$$k = \left(\frac{1}{0.002}\right)^n R_{p0.2} \tag{4}$$

The mean values the percentage elongation after fracture A_{mean}, the strain-hardening exponents n_{mean} and the strength coefficients k_{mean} are then determined analogous to the Eq. (1). The experimental data and the calculated data for the material model based on the tensile tests results by various test temperatures T are presented in Tables 1–3.

The values of Young's modulus E by various testing temperatures are defined for the molybdenum according the Plansee data [28] in Fig. 9 and collected in Table 4.

The 2D model is built in Marc/Mentat software and it consists from one meshed contact body – the molybdenum strip and rigid bodies representing the holder, bending and guiding cylinders described above (Fig. 7). The device strip slot was also modeled to check the interference between the molybdenum strip and the device body during the test procedure at the holder cylinder penetration of 6 mm as shown in detail in Fig. 10.

The simulations were done by the same conditions as the strip tests. The drawbead height was simulated by pressing the holder cylinder into the strip during the first 10 s of the simulation. This loadcase was followed by pulling the strip through the device cylinders during next 50 s by the constant velocity of 30 mm s^{-1}.

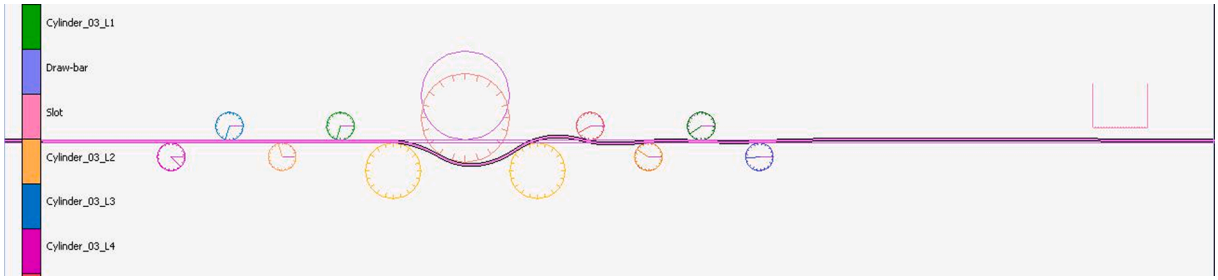

Fig. 10. Detail of Baosteel/Sanchez experiment 2D FEM model.

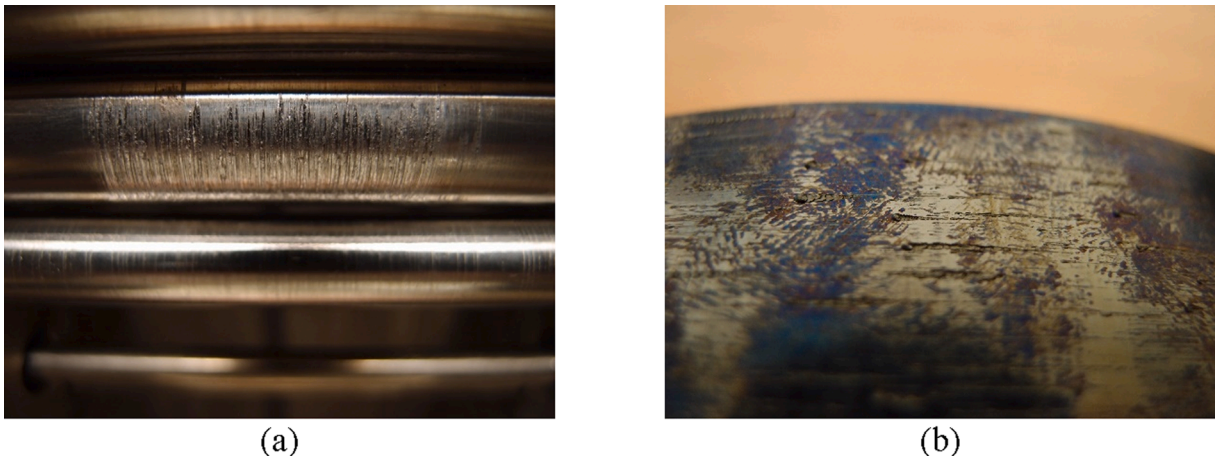

Fig. 11. Detail of the damage during the test procedure without lubricant by T = 320 °C: (a) fixed cylinder; (b) molybdenum strip.

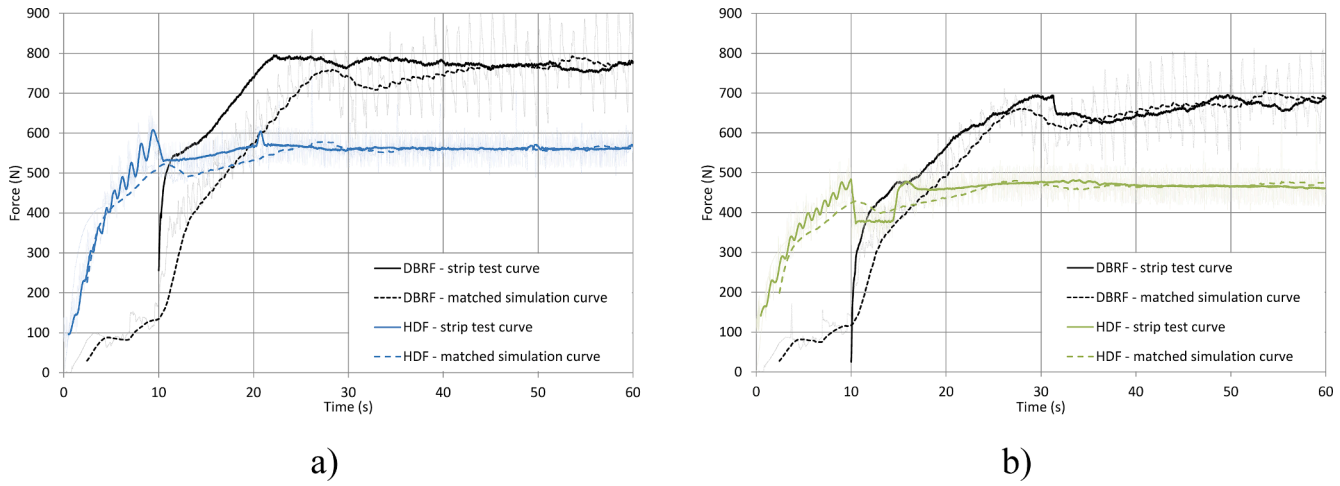

Fig. 12. Strip test and matched simulation HDF and DBRF curves after the test procedure without lubricant: a) $H = 4$ mm, $T = 20$ °C; b) $H = 4$ mm, $T = 120$ °C.

4. Data processing

The simulations were done by the same conditions as the strip tests. The drawbead height was simulated by pressing the holder cylinder into the strip during the first 10 s of the simulation. This loadcase was followed by pulling the strip through the device cylinders during next 50 s by the constant velocity of 30 mm.s^{-1}.

The inverse method of the friction coefficient calculation was done using the Coulomb bilinear friction model used also by Meng et al. [15]. The value of the friction coefficient was changed in steps of 0.01 to match the simulation results of the DBRF and HDF progress with the results of the performed strip tests.

4.1. Dry surfaces friction coefficient matching

The dry surface friction coefficient state was tested only by the 4 mm drawbead hight to prove the accuracy of the chosen methodology. Because of the wear of the fixed cylinder in the test device induced by the permeation of the molybdenum sintered strip blank sliding through it under dry condition by the temperature $T = 320$ °C, the results of the experiments without lubricant are presented only for the temperatures $T = 20$ °C and 120 °C and the drawbead height $H = 4$ mm. The damage of the fixed cylinder and the blank strip upper layer occurred by the temperature $T = 320$ °C is shown in Fig. 11. After this damage occurrence, next strip tests with dry surfaces were cancelled.

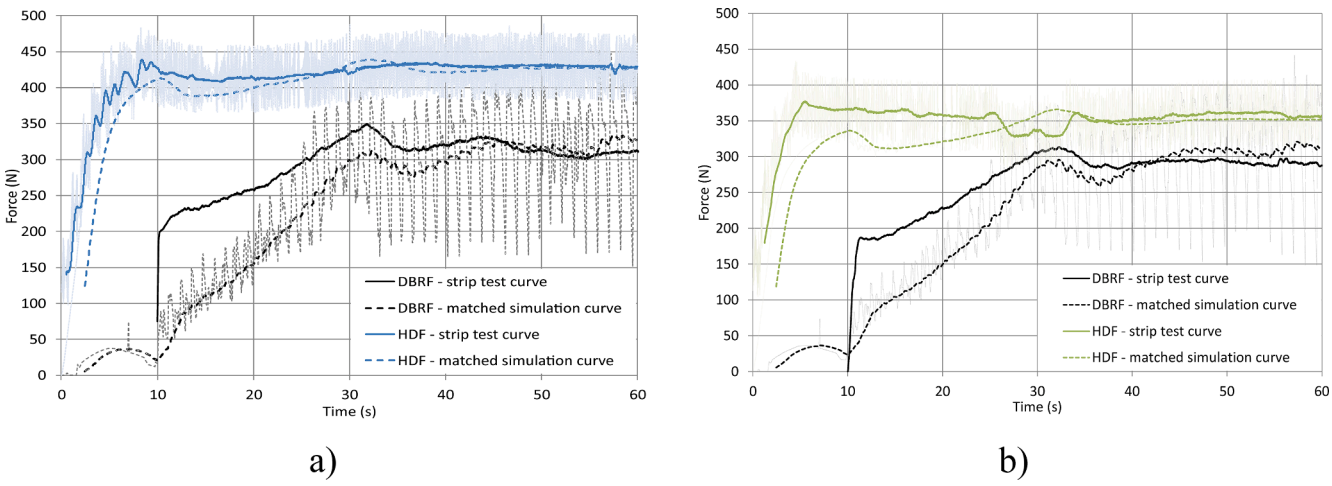

Fig. 13. Strip test and matched simulation HDF and DBRF curves after the test procedure with lubricant: a) $H = 2$ mm, $T = 20$ °C; b) $H = 2$ mm, $T = 120$ °C.

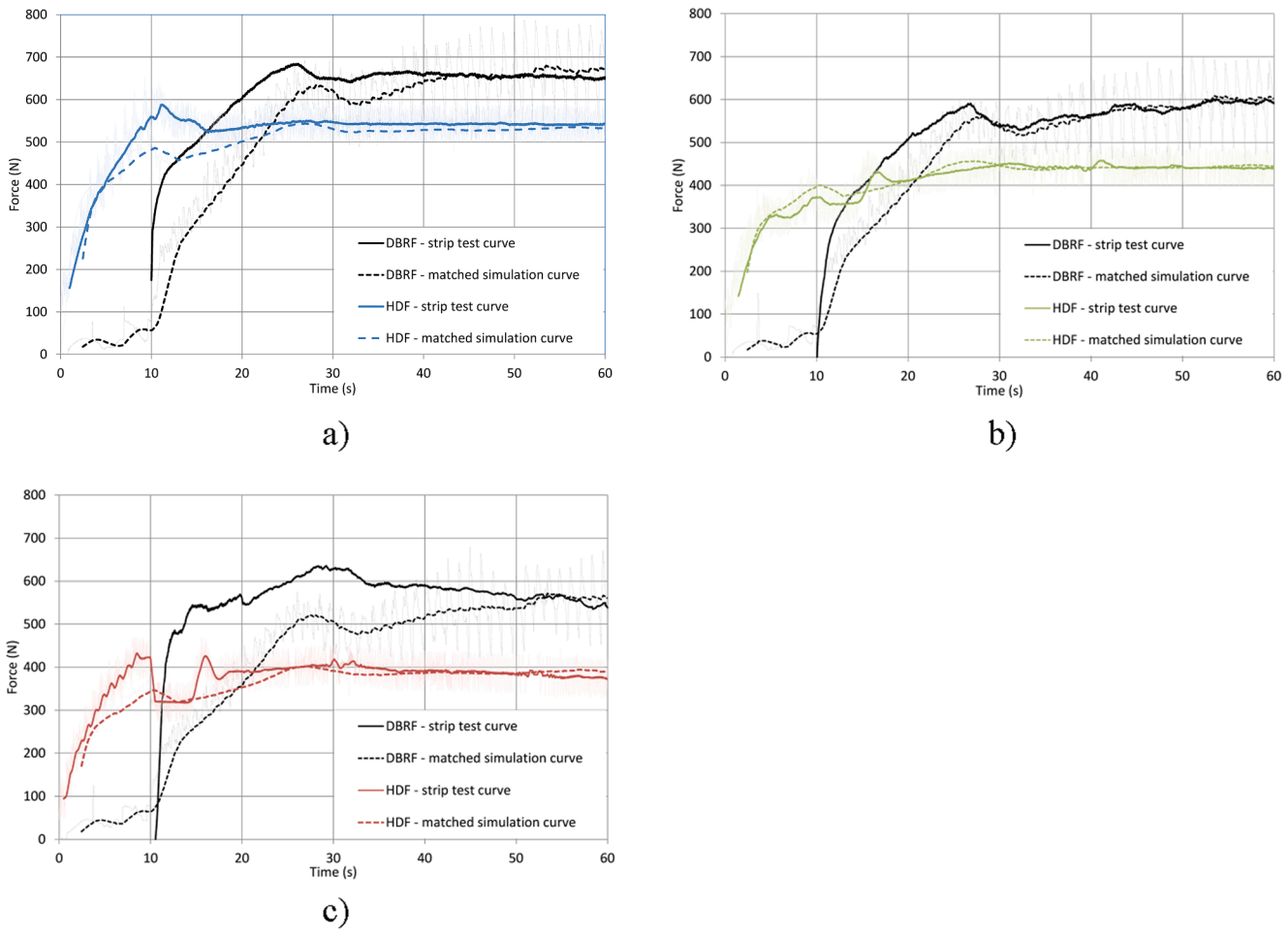

Fig. 14. Strip test and matched simulation HDF and DBRF curves after the test procedure with lubricant: a) $H = 4$ mm, $T = 20$ °C; b) $H = 4$ mm, $T = 120$ °C; c) $H = 4$ mm, $T = 320$ °C.

Fluctuating data curves from the tests and force curve matching simulations were replaced by the trend lines calculated by the moving average method with the 50 data points period. The results of the experimental and simulation data match show the drop of the HDF and DBRF by the temperature $T = 120$ °C towards the initial test temperature $T = 20$ °C by the constant drawbead height $H = 4$ mm (Fig. 12). It is caused by the decrease of yield strength of molybdenum strip at elevated temperature. Best match of the HDF and DBRF curves by dry contact surfaces was obtained by the friction coefficients $f = 0.1$ for $T = 20$ °C and $f = 0.11$ for $T = 120$ °C. The increase of the friction coefficient is caused by the increase of the surface contact between molybdenum sheet and the testing tool.

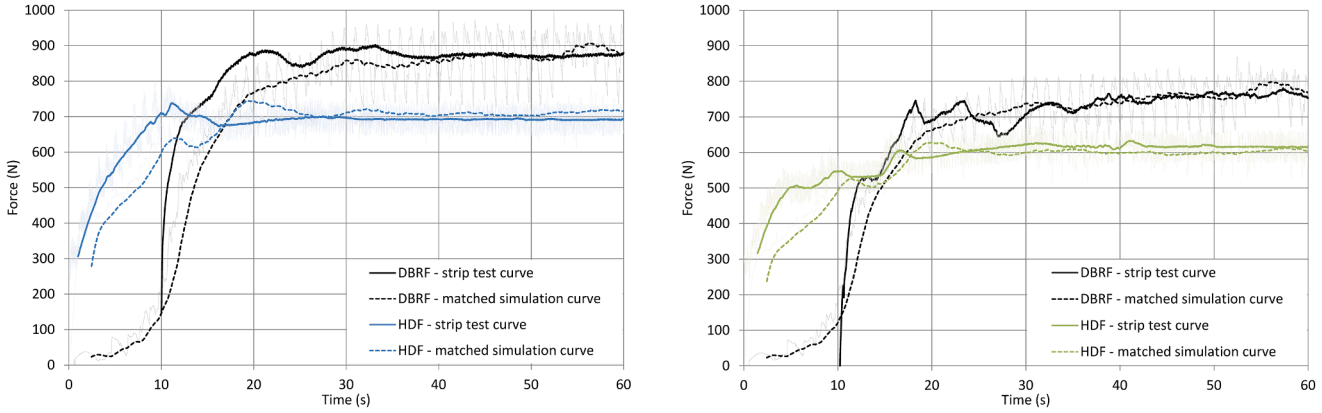

Fig. 15. Strip test and matched simulation HDF and DBRF curves after the test procedure with lubricant: a) $H = 6$ mm, $T = 20$ °C; b) $H = 6$ mm, $T = 120$ °C.

Table 5
Friction coefficients between lubricated molybdenum strip and steel cylinders by various temperatures and drawbead heights.

Testing temperature T (°C)	Friction coefficients f (-)
20	0.02
120	0.03
320	0.06*

* Performed only by the drawbeadhight $H = 4$ mm.

4.2. Lubricated surfaces friction coefficient matching

The tests with various drawbead hight and lubricated blank were performed after replacement of the damaged fixed cylinder of the test device. The results of the simulations and the tests are shown for various conditions in Figs. 13–15 for lubricated cylinders. Fluctuating data curves from the tests and calculations were replaced by the trend lines calculated by the moving average method with the 50 data points period.

The results show the drop of the HDF and DBRF by all drawbead heights by rising the temperature to $T = 320$ °C for the drawbead height $H = 4$ mm and to $T = 120$ °C for the drawbead heights $H = 2$ mm and 6 mm. The values of the friction coefficients acquired by lubricated contact surfaces for tested drawbead hights and temperatures are presented in Table 5.

5. Conclusion

This research investigated the frictional characteristic of molybdenum strips at elevated temperature. The inverse comparison method was utilized to obtain the coefficients of friction (COF) for further deep drawing simulations of molybdenum containers for sapphire crystals produced by the Bagdasarov method and next development of a mechatronic deformation system. A series of uniaxial tests by various temperatures were done to obtain the data for the simulation material model building. The uniaxial tests were followed by the strip tests performed by the same temperatures by various drawbead heights and dry and lubricated surfaces of the blank and the fixed cylinders of the test device. A simple 2D strip test simulation model was built using the friction bilinear model.

The holder drawing force (HDF) and the drawbead restraint force (DBRF), which were measured by the strip test and also observed by the simulation procedures, are influenced by the coefficient of friction (COF) between the strip test device cylinders and the molybdenum strip specimen. The magnitude and the shape of the obtained HDF and DBRF is in the relationship with the COF at a particular testing temperature. Using the inverse comparison approach, the coefficient of friction at a certain temperature was obtained via matching the HDF and BDRF simulation curves to the ones measured by the strip tests. The increasing testing temperature of molybdenum strips led to reduced HDF and DBRF values and increased friction coefficient, so the testing temperature and lubricant are the factors affecting the coefficient of friction and also the strip test measured forces.

The strip test by the dry conditions were done only for one drawbead height by the temperatures $T = 20$ °C and 120 °C because of the damage occurred on the fixed cylinder and the molybdenum specimen by the temperature $T = 320$ °C. The damage caused the rupture of the upper layer of the molybdenum strip produced by the sintered carbide technology, which scratched subsequently the fixed cylinder of the test device. The values of COF by dry conditions were stated for the drawbead height $H = 4$ mm to $f = 0.1$ for $T = 20$ °C and $f = 0.11$ for $T = 120$ °C.

After replacement of the damaged fixed cylinder in the test device, there were determined friction coefficients between lubricated molybdenum strips and fixed steel cylinders at the temperature ranging from 20 °C to 320 °C. The test by the temperature $T = 320$ °C was performed just for the drawbead height $H = 4$ mm, which will be used by container deep drawing simulations following the work of Zmindak et al. [11]. The value of the coefficient of friction by lubricated surfaces of the test cylinder and the molybdenum blank was stated to 0.02 at 20 °C, raising to 0.03 at 120 °C and 0.06 at 320 °C in a non-linear sequence.

The coefficient of friction of pure molybdenum sheet increased with rising temperature by dry and by lubricated surfaces too. The drawbead restraint forces (DBRF) and also the holder drawing forces (HDF) decreased with rising temperature by dry and by lubricated surfaces too. Such conclusion was expected taking into account the results of the tests done by the temperatures from 720 °C to 870 °C in the vacuum by Meng et al. [15]. The observed relation is attributed to the decrease of yield strength of molybdenum strip (BDRF and HDF decrease) and the increase of surface contact between molybdenum sheet and tooling (COF increase) at elevated temperature. The influence of the drawbead height to the COF value was not observed by its change with the step set to 0.01 during the simulation data matching process.

The results of the experiments and calculations will be used by further development and FEA simulations of a molybdenum crucible mechatronic deep drawing system [29–31] using the computer control of the blankholder and drawbeads to test various control strategies of the molybdenum container deep drawing process.

CRediT authorship contribution statement

Frantisek Brumercik: Conceptualization, Methodology, Writing - original draft, Software, Data curation, Supervision. **Ronald**

Bastovansky: Formal analysis, Investigation, Data curation. **Michal Lukac:** Visualization, Investigation, Software. **Adam Glowacz:** Writing - review & editing, Resources, Validation.

Declaration of Competing Interest

The authors declare that they have no known competing financial interests or personal relationships that could have appeared to influence the work reported in this paper.

Acknowledgements

The research is supported by the Cultural and Educational Grant Agency of the Ministry of Education, Science, Research and Sport of the Slovak Republic under the project KEGA 046ŽU-4/2018.

References

[1] M. Martikan, F. Brumercik, R. Bastovansky, Development of mechatronic deformation system, Appl. Mech. Mater. 803 (2015) 173–178, https://doi.org/10.4028/www.scientific.net/AMM.803.173.
[2] R. Bastovansky, M. Tropp, M. Lukac, F. Brumercik, Molybdenum sheet metal test device, Communications – Scientific Lett. Univ. Zilina 19 (2017) 124–127.
[3] Q. Zhu, M. Xie, X. Shang, G. An, J. Sun, N. Wang, S. Xi, Ch. Bu, J. Zhang, Research status and progress of welding technologies for molybdenum and molybdenum alloys, Metals 10 (2020) 279, https://doi.org/10.3390/met10020279.
[4] T. Trzepiecinski, Recent developments and trends in sheet metal forming, Metals 10 (2020) 779, https://doi.org/10.3390/met10060779.
[5] J. Kajan, M. Volkov, G. Damazyan, I. Mukhin, T. Gregor, O. Palashov, Fabrication and characterization of high-dimension single-crystal Yb:YAG ingots grown by horizontal directed crystallization method, Crystal Res. Technol. (2020), https://doi.org/10.1002/crat.202000105, 2000105.
[6] B. Meng, M. Wan, X. Wu, Y. Zhou, Development of thermal deep drawing system with vacuum environment for difficult-to-deformation materials, Trans. Nonferrous Met. Soc. China 22 (2012) 254–260, https://doi.org/10.1016/S1003-6326(12)61716-6.
[7] B. Meng, M. Wan, X. Wu, Y. Zhou, Ch. Chang, Constitutive modeling for high-temperature tensile deformation behavior of pure molybdenum considering strain effects, Int. J. Refractory Metals Hard Mater. 45 (2014) 41–47, https://doi.org/10.1016/j.ijrmhm.2014.03.005.
[8] E.A. Nazaryan, M.M. Arakelyan, Technologie of drawing of molybdenum sheet for growing single crystals, IX International congress machines, technologies, materials, September 19 – 21 2012 Varna, Bulgaria. 9–11.
[9] H. Livatyali, M. Firat, B. Gurler, M. Ozsoy, An experimental analysis of drawing characteristics of a dual-phase steel through a round drawbead, Mater. Des. 31 (2010) 1639–1643, https://doi.org/10.1016/j.matdes.2009.08.030.
[10] M. Mitka, R. Bastovansky, F. Brumercik, P. Ignaciuk, Local resistance of heating molybdenum sheet in a test device, Adv. Sci. Technol. Res. J. 11 (2017) 87–93, https://doi.org/10.1088/1757-899x/159/1/012008.
[11] M. Zmindak, T. Donic, P. Jurik, Numerical simulation of rectangular deep draw containers made from thin molybdenum sheet, IOP Conf. Series Mater. Sci. Eng. 159 (2016), 012008, https://doi.org/10.1088/1757-899X/159/1/012008.
[12] C. Thiebaut, C. Bonnet, J.M. Morey, Evolution of the friction factor of a molybdenum workpiece during upsetting tests at different temperatures, J. Mater. Process. Technol. 77 (1998) 240–245, https://doi.org/10.1016/S0924-0136(97)00423-8.
[13] N. Arab, E.A. Nazaryan, M. Arakelyan, Investigation to production molybdenum container to growth single crystals by deep drawing process, Int. J. Mech. Mater. Eng. (IJMME) 5 (2010) 116–122.
[14] Z. Lin, Ch. Chen, Inverse calculation of the friction coefficient during the warm upsetting of molybdenum, Int. J. Mech. Sci. 47 (2005) 1059–1078, https://doi.org/10.1016/j.ijmecsci.2005.02.009.
[15] B. Meng, M.W. Fu, M. Wan, Drawability and frictional behavior of pure molybdenum sheet in deep-drawing process at elevated temperature, Int. J. Adv. Manuf. Technol. 78 (2015) 1005–1014, https://doi.org/10.1007/s00170-014-6698-2.
[16] W.F. Hosford, R.M. Caddell, Metal Forming Mechanics and Metallurgy, third ed., Cambridge University Press, New York, 2007.
[17] V.N. Korolev, L.A. Shofman, Deep drawing of molybdenum and its alloys, Forging and stamping 10 (1967) 17–23.
[18] H.D. Nine, Drawbead forces in sheet metal forming, in: D.P. Koistinen, N.M. Wang (Eds.), Mechanics of Sheet Metal Forming, Springer Boston, MA, USA, 1978, pp. 179–211.
[19] T. Trzepiecinski, A. Kubi, J. Slota, R. Fejkiel, An experimental study of the frictional properties of steel sheets using the drawbead simulator test, Materials. 12 (24) (2019) 4037, https://doi.org/10.3390/ma12244037.
[20] T. Trzepiecinski, H.G. Lemu, Recent developments and trends in the friction testing for conventional sheet metal forming and incremental sheet forming, Metals. 10 (1) (2020) 47, https://doi.org/10.3390/met10010047.
[21] S. Leocata, t. Senner, H. Reith, A. Brosius, Experimental analysis and modeling of friction in sheet metal forming considering the influence of drawbeads, Int. J. Adv. Manuf. Technol. 106 (2020) 4011–402. https://doi.org/10.1007/s00170-019-04847-z.
[22] J. Machalek, Projects of progressive production technologies of parts from sheet-metal with the use of finite elements method Dissertation thesis, Ostrava, 2012.
[23] GLEIT-μ® HP 516 Weiße Paste für die Heißformung. http://www.wessely.co.at/de/produkte/hochleistungspasten/item/38-hp516-weisse-paste-fuer-heissformung.html, 2020 (accessed 30 June 2020).
[24] H.-K. Kim, S.K. Hong, FEM-based optimum design of multi-stage deep drawing process of molybdenum sheet, J. Mater. Process. Technol. 184 (2007) 354–362, https://doi.org/10.1016/j.jmatprotec.2006.12.001.
[25] J. Cheng, S. Nemat-Nasser, W. Guo, A unified constitutive model for strain-rate and temperature dependent behavior of molybdenum, Mech. Mater. 33 (2001) 603–616, https://doi.org/10.1016/S0167-6636(01)00076-X.
[26] T. Trzepiecinski, Numerical modeling of the drawbead simulator test, Zeszyty naukowe politechniki rzeszowskiej, Mechanika z. 84 (2012) 69–78, https://doi.org/10.7862/rm.2012.6.
[27] Z. Zhang, Q. Sun, Ch. Li, W. Zhao, Theoretical calculation of the strain-hardening exponent and the strength coefficient of metallic materials, J. Mater. Eng. Perform. 15 (2006) 19–22, https://doi.org/10.1361/10599490524057.
[28] Modulus of elasticity of molybdenum plotted against the testing temperature compared to our other refractory metals: tungsten, tantalum and niobium. https://www.plansee.com/en/materials/molybdenum.html, 2020 (accessed 30 June 2020).
[29] M. Tropp, M. Tomasikova, R. Bastovansky, L. Krzywonos, F. Brumercik, Concept of deep drawing mechatronic system working in extreme conditions, Procedia Eng. 192 (2017) 893–898, https://doi.org/10.1016/j.proeng.2017.06.154.
[30] M. Tropp, M. Tomasikova, R. Bastovansky, L. Krzywonos, F. Brumercik, Z. Krzysiak, Transient thermal simulation of working components of mechatronic system for deep drawing of molybdenum sheets, in: D. Herak (Ed.) Proceedings of 58th international conference of machine design departments (ICMD 2017), 2017, pp. 408–413. https://doi.org/10.1088/1757-899X/393/1/012075.
[31] M. Tropp, M. Lukac, M. Benko, F. Brumercik, Z. Krzysiak, A. Nieoczym, Sealing technology for vacuum applications working by increased temperatures, in: S. Medvecky, S. Hrcek, R. Kohar, F. Brumercik, V. Konstantova (Eds.) Current Methods of Construction Design: Proceedings of the ICMD 2018, Springer Nature Switzerland, 2020, pp. 185–192, https://doi.org/10.1007/978-3-030-33146-7.